EXPERIMENTAL INVESTIGATION OF DELTA WING FLOW BEHAVIOUR UNDER PITCHING MOTION

M. Z. A. D. Huri,[a] S. Mat,[a,*]

[a] Faculty of Mechanical Engineering,
Universiti Teknologi Malaysia,
81310 Skudai, Johor Darul Ta'zim.

Article history
Received
28 October 2015
Received in revised form
6 November 2015
Accepted
11 December 2015

*Corresponding author
shabudin@fkm.utm.my

GRAPHICAL ABSTRACT

ABSTRACT

This paper presents an experimental study of delta wing flow behaviour under pitching motion. The aim is to investigate the pressure distribution of the flow over sharp-edged delta wing. The flow behaviour over the upper surface of a delta wing is mainly governed by the leading edge vortices. Angle of attack variation is applied to simulate the pitching motion of the delta wing. The project focuses on estimating the pressure distribution for a sharp-edged delta wing with 65o sweep angle. Wind tunnel testing is done at two flow velocities, which are 13.5 m/s and 15 m/s. The trend of pressure coefficient (cp) against the spanwise location is then analysed based on four aspects, which are the variations of Reynolds number, chordwise location, spanwise location and angle of attack. The results show that the pressure at the vicinity of leading edge is much lower than the pressure plotted near to the wing centre.

KEYWORDS

Delta wing; pitching; vortex

INTRODUCTION

Delta wing is commonly applied in the design of supersonic aircraft wing. This special case of swept wing is basically in triangular shape plan form [1]. Among the famous aircrafts that have delta wing are the USAF fighter aircraft and Convair F-102A. In reality, aircrafts with delta wing fly at subsonic speed most of the time and only reach supersonic speed for intended purposes as it requires more power. The aerodynamics characteristics of delta wing majorly rely on the primary and secondary vortices which form at the verge of the leading edges, or known as leading edge vortices, as shown in Figure 1.

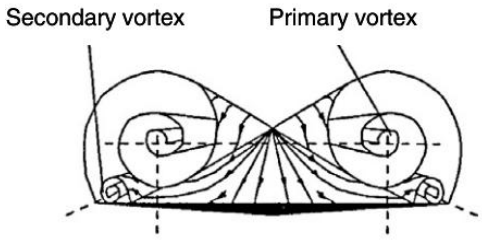

Figure 1: Schematic view of flow-field over delta wing [2]

The flow over delta wing can simply be described as a flow with a spiral type motion from the lower to upper surface of the delta wing [3]. Flow separation either occurs at the leading edge forms the primary vortex or due to the interaction of primary vortex with the boundary layer on the wing surface, creating secondary vortex.

Subsonic flow over delta wing creates a pressure distribution that contributes to the lift force of the wing. The pressure distribution on the wing helps

in enhancing the formation of leading edge vortices. Figure 2 shows the pressure distribution over the delta wing upper and lower surfaces.

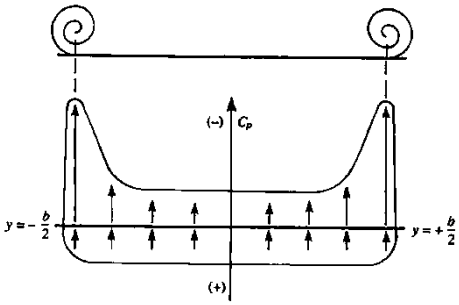

Figure 2: Delta wing pressure distribution [1]

From the figure, near to the leading edge, the local static pressure is relatively small. Thus, the pressure is reduced at the vicinity of the leading edge to be considerably constant over the middle section of the wing [1]. The variation of pressure coefficient is as shown in Figure 2 above in the spanwise direction. On the bottom surface of the wing, the pressure is reasonably constant. A suction effect is created on the top surface near the leading edges, which enhances the lift of the wing.

The strength of the lift-enhancing wing vortices will increase with increasing angle of attack until a vortex breakdown occurs, which is actually a sudden disorganization of flow [4]. Vortex breakdown of a flow over delta wing commonly occurs at a location about two-thirds of the wing chord [1]. Vortex breakdown is associated with the flow separation resulting from the influence of adverse pressure gradient.

Modification Of Model

This project involves the fabrication of the sharp-edged delta wing model to be suited with the pitching motion mechanism.

Pitching Mechanism

Figure 3 shows the overall structure of the delta wing pitching motion mechanism for the experiment. The structure consisted of a main curved column, a motor system and a pitching arm which held and connected the model to the curved column.

Pitching motion of the delta wing was controlled by the gear mechanism. The motor would rotate the gear to roll and push the arm attached with the model down and up the reel designated on the curved column with radius of 2.05 meter. As the gear would roll down the column, it would push the arm upward and hence the delta wing model would pitch up about the radius centre, and vice versa for pitch down motion.

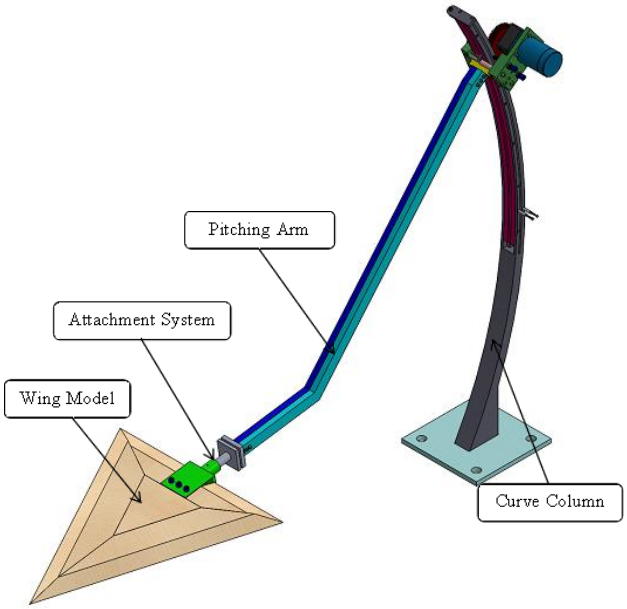

Figure 3: Overall structure of the pitching mechanism

Delta Wing Model

The model as shown in Figure 4 was made from wood. It consisted of four main parts, which were left and right leading edges, trailing edge and centre section to completely form a 65° swept delta wing. A total of 30 pressure taps installed were divided and arranged into two lines, which were line A and line B, with 15 taps inserted at each line, as presented in Figure 4.

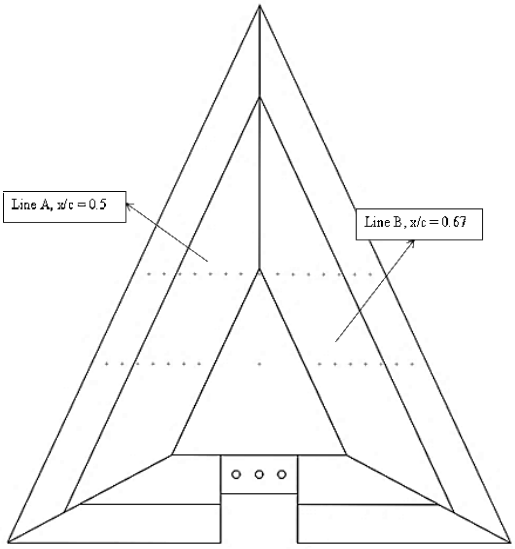

Figure 4: Overall structure of the pitching mechanism

WIND TUNNEL TEST

The experiment of delta wing under pitching motion was conducted in UTM Low Speed Wind Tunnel facility (UTM-LST) available at Universiti Teknologi Malaysia Aeronautics Laboratory (Aerolab).

Fitting Of Pitching Mechanism

The side view of the overall pitching mechanism is shown in Figure 5. The overall structure of the pitching mechanism was installed in the wind tunnel test section with dimension of 2.0 m (width) x 1.5 m (height) x 5.8 m (long).

Figure 5: The structure viewed from side of the test section

Test Configurations

Two values of flow velocities involved were 13.5 m/s and 15 m/s. Due to limitation in terms of the strength of the pitching arm, the maximum velocity that the structure could withstand was only 15 m/s. Further increment in flow velocity would cause the structure to fail. Six degrees of angle of attack, from 0^o, 5^o, 8^o, 10^o, 15^o, and 17^o, respectively, were varied in ascending order.

The approximation of the Reynolds number was calculated based on the wing chord length (0.7m). The Reynolds numbers involved in this experiment with their respective flow velocity is presented in Table 1.

Table 1: Reynolds number based on 0.7m chord

Flow Velocity, V∞ (m/s)	Reynolds Number, Re
13.5	0.75×10^6
15	0.85×10^6

RESULTS AND DISCUSSION

Variation of Reynolds Number

Figure 6 shows the trend of pressure coefficient (Cp) in spanwise direction with varying angle of attack. Figure 6(a) presents the pressure distribution at 13.5 m/s flow velocity and Figure 6(b) presents the pressure distribution at 15 m/s.

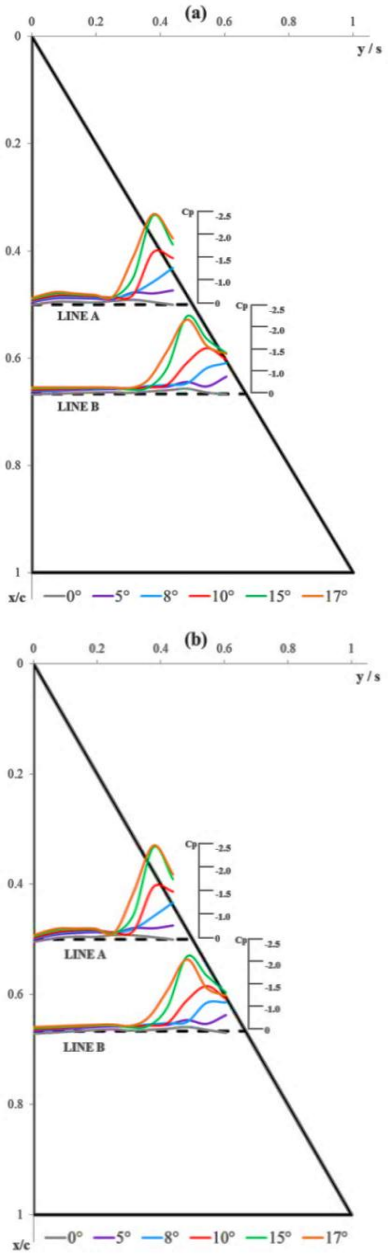

Figure 6: Half-span pressure distribution (a) 13.5 m/s (b) 15 m/s

The Cp was plotted at two different chordwise locations; Line A (0.5c) and Line B (0.67c) respectively. Generally, the trend of Cp for both velocities was similar with the peak pressure at 0.5c at about -2.5 Cp for 17^o angle of attack. At

Line B on both velocities, the peak pressure at 15° was higher than 17° with Cp value ranging from -2.2 to -2.4. The pressure decreased rapidly at y/s = 0.25 for both flow velocities at 0.5c chordwise location. Meanwhile, for 0.67c location, the decrease of pressure began at y/s = 0.35. At lower angle of attack (0° to 8°), the peak Cp was less than those at higher angle of attack (10° and 17°).

Pressure distributions at 13.5 m/s and 15 m/s were created a Cp trend with small deviation from one to another. Therefore, from this particular experimental study, the variation of Reynolds number would give no significant change in pressure distribution on the surface pressure of the delta wing. High suction peaks were found at the vicinity of leading edge because of the formation of the vortex core [5]. Towards the wing root chord, the peak pressure was relatively reduced.

Variation of Spanwise Location

The experimental results of Cp trends on full wing span at 0.5c and 0.67c are presented in Figure 7 and Figure 8, respectively. The presented data is the pressure distribution at flow velocity of 13.5 m/s with different angle of attack.

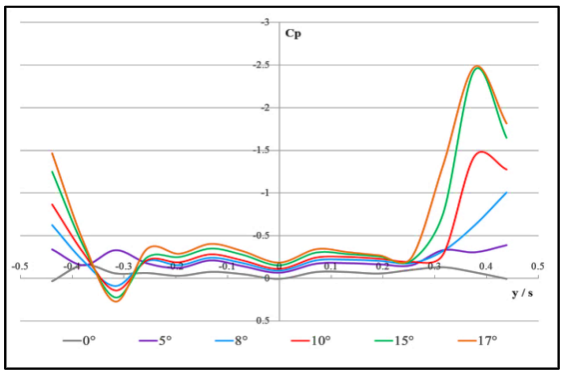

Figure 7: Spanwise pressure distribution at 0.5c (Line A)

Referring to Figure 7, the plotted pressure distribution is different between the left and right side of the delta wing. Negative range of y/s represents the wing left side, and the right side of the wing is represented by positive y/s range. The peak pressure at positive y/s occurred at -2.5 Cp value when the angle of attack was 17° whereas the peak value of pressure at the left side was about 0.25 Cp. For positive y/s, the pressure decreased rapidly starting from y/s = 0.25 until it reached the peak value. Contrary to the right side, the pressure at negative y/s value increased gradually to the peak Cp. This obvious difference in Cp trend between the left and right side of the wing was observed to be consistent from 8° to 17° angle of attack.

The difference of pressure trend observed between the right and left wing side was analysed to be a consistent technical error. This error was observed occurring at spanwise location of y/s = -0.316. The installed pressure tap at this spanwise location was found to have a blockage, and thus it read set of invalid pressure values. The cause of the blockage was yet to be figured out but it was confirmed to be at some position within the tube inside the wing model.

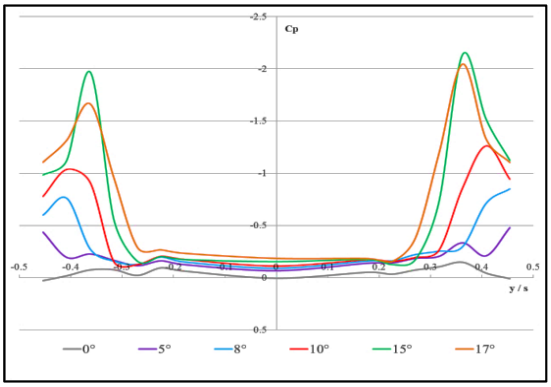

Figure 8: Spanwise pressure distribution at 0.67c (Line B)

The chordwise location of 0.67c created similar trend of Cp over the model upper surface with high peak pressure occurrence near to the leading edge, and the peak pressure close to the wing root chord was comparatively lower. However, the peak values at different angle of attack were found to be different between the right and left sides of the span. The highest peak values for both sides occurred at 17° angle of attack but for the right side (y/s > 0) the peak Cp value was at -2.15, whereas the peak Cp value for negative y/s range was at -1.95. Generally, peak values at different angle of attack for the left side of the wing would be lower than those at the right side with 20% average difference.

Dissimilarity of the pressure values between the left and right of the wing might be due to the roughness of wing upper surface. The wing model was made from wood, hence after some machining and fabrication processes, the surface roughness became reasonably high. Poor and inconsistent surface finishing on the wing upper surface might have led to this difference of pressure reading at different spanwise locations. If surface roughness was the cause of the difference, surface at the left side of the wing could be said to be smoother than the right side surface. Smoother surface will allow the flow to be less attached, thus

increasing the local flow velocity and delivering lower static pressure.

Variation of Chordwise Location

This section presents analysis on the pressure distribution at different chord wise location, which were at 0.5c and 0.67c. Line A station represents 0.5c chordwise location, whereas Line B symbolizes the 0.67c. The results would be shown at two different angles of attack, 10° and 17°. Flow velocity was fixed at 13.5 m/s as Reynolds number would give no significant effect on the flow. The trend of Cp against spanwise location had been analysed and discussed in terms of its similarities and differences.

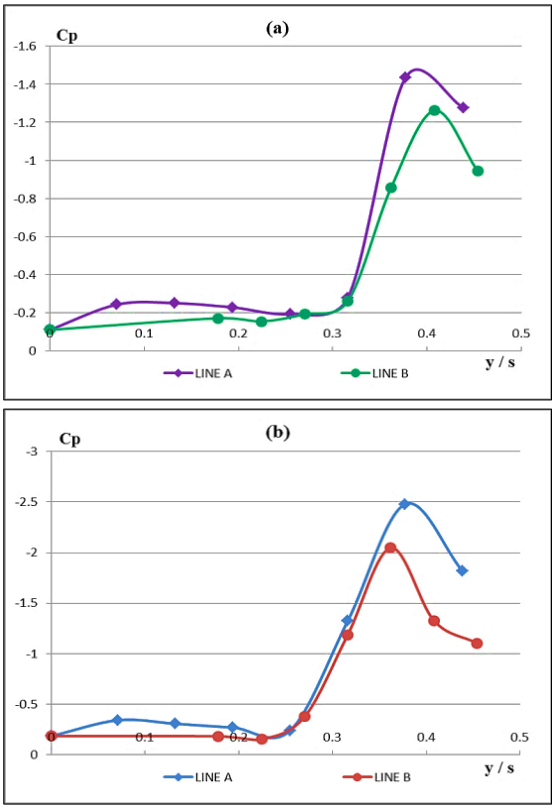

Figure 9: Spanwise pressure distribution at different chordwise stations (a) α = 10° (b) α = 17°

Figure 9 (a) shows the pressure trend at two different chordwise locations for 10° angle of attack. The peak pressure value was found to be lower at Line A with Cp = -1.45 compared to peak value of Cp = -1.26 at Line B. At Line A, the peak pressure occurred at y/s = 0.38, while the peak pressure occurred at y/s = 0.4 for Line B. The gradient in decrease of pressure was steeper at 0.5 of chord. Both stations had similar trend with low pressure value near the leading edge and comparatively high value towards the middle wing section.

As seen in Figure 9 (b), similar pressure distribution was obtained at both chordwise locations. As plotted for 10° angle of attack, peak Cp value was higher at Line A compared to Line B with respective Cp value of -2.5 and -2.05. The spanwise locations of the highest peak value were similar as before. The Cp trend for 17° angle of attack was also analogous to the Cp trend plotted for 10° angle of attack. Adverse pressure gradient was obviously formed within y/s = 0.23 to y/s = 0.38, which displayed a similar stiffness.

For both angles of attack (10° and 17°), the trends of pressure against the spanwise location were basically similar although plotted at two different chordwise locations. Low pressure zone was created near the leading edge with highest peak value occurrence within y/s = 0.38 to y/s = 0.4. The peak pressure value was higher at 50% chord compared to 67% chord. The magnitude of static pressure decreased as the trailing edge of the wing was approached [5]. The decrease in pressure with respect to the chordwise location might have corresponded to the decrease in vortex strength.

Variation of Angle Of Attack

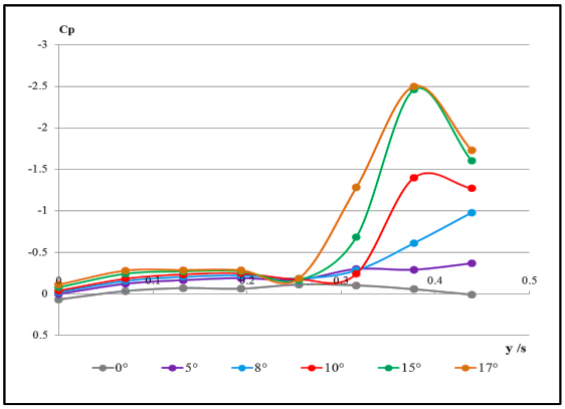

Figure 10: Spanwise pressure distribution at 0.5c

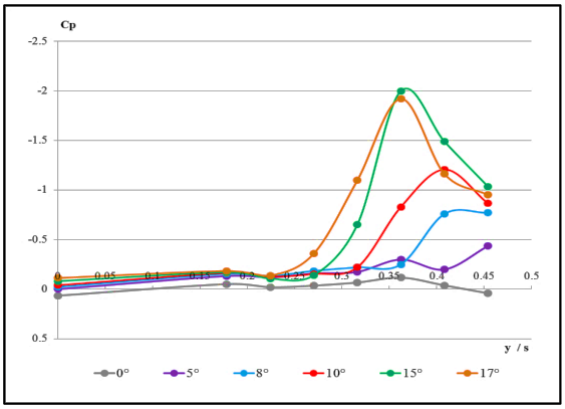

Figure 11: Spanwise pressure distribution at 0.67c

The experiment was conducted by increasing the angle of attack from 0^o to 17^o. The increment of angle of attack of the wing model would simulate the pitching motion. Figure 10 shows the Cp trend against spanwise locations at 0.5c chordwise location, while Figure 11 displays the pressure distribution at 0.67c. Both results were based on 15 m/s flow velocity at different angle of attack which were 0^o, 5^o, 8^o, 10^o, 15^o and 17^o respectively.

Referring to Figure 10, the magnitude of the peak pressure gradually increased as the angle of attack increased. Highest peak value of Cp occurred at 17^o angle of attack with Cp equal to -2.5. The pressure began to decrease rapidly within 0.22 to 0.25 y/s spanwise location. For angle of attack ranging from 10^o to 17^o, the Cp value decreased until a certain value at y/s = 0.37, before it rose again, creating an adverse pressure gradient.

As seen in Figure 11, similar pressure trends were observed at 0.67c chordwise location. However, the highest peak pressure occurred at 15^o angle of attack with Cp equal to -2.0. The mean pressure coefficient at 0^o angle of attack at 0.67c was higher than at 0.5c chordwise location. The Cp value at angle of attack ranging from 10^o to 17^o also decreased until it reached a peak value before increasing similarly as plotted for 0.5c station, but peak pressure for 10^o angle of attack at 0.67c occurred at y/s = 0.4. The mean peak value of pressure coefficient obtained at 0.67c was lower than 0.5c chordwise station.

At both chordwise locations, the peak pressure began to be noticeable at 5^o angle of attack, meaning that the leading edge flow separation occurred at low angle of attack. High peak pressure was recorded near to the leading edge as compared to the region close to the root chord. This signified the formation of vortex core near the leading edge and a potential flow formed at the middle section of the wing [6] with higher and considerably constant pressure.

CONCLUSION

Pressure distribution of the flow over the sharp-edged delta wing has been analyzed through four different aspects, which are variation of Reynolds number, spanwise location, chordwise location and angle of attack. From the results of this study, it is found that the change on Reynolds number gives no significant on the pressure distribution. The trend of pressure in spanwise location is found to be not symmetrical although the upper surface of the wing is symmetrical around the chord. The difference in chordwise pressure distribution in this study may be due to some technical errors on the wing model, which requires further investigation to verify problem.

The variation in terms of chordwise location has revealed that the surface pressure decreases as the flow approaches the trailing edge of the wing. Increasing the angle of attack simulates the pitching up motion of the wing. As the wing pitches up, the low pressure region near the leading edge also increases. The decrease in pressure value with respect to the increase in angle of attack may correspond to the increase of leading edge vortex strength. Generally, low pressure occurs at the vicinity of the leading edge and it increases towards the middle wing section. The pressure distribution recorded in this study signifies the vortex core formation close to the leading edge.

REFERENCES

[1] *Anderson, J. J. D. 2011. FUNDAMENTALS OF AERODYNAMICS FIFTH EDITION IN SI UNITS. 895-898, 464-475.*

[2] *Schutte, A., & Ludeke, H. 2013. Numerical investigations on the VFE-2 65-degree rounded leading edge delta wing using the unstructured DLR TAU-Code. Aerospace Science and Technology, 24, 56-65.*

[3] *Coton, F. N., Mat, S. B., Galbraith, R. A. M., & Gilmour, R. 2008. Low Speed Wind Tunnel Characterization Of The VFE- 2 Wing. American Institute of Aeronautics and Astronautics, Vol. 48.*

[4] *Gortz, S. 2005. Realistic Simulations of Delta Wing Aerodynamics using Novel CFD Methods. KTH Aeronautical and Vehicle Engineering, 1-84.*

[5] *Sun, Y. C. 1957. Experimental Investigation of the Flow Field about Sharp-Edged Delta and Rectangular Wings. Bachelor thesis.*

[6] *M, G., & Parammasivam, K. M. 2006. Pressure Measurements on Delta wing with different leading edge radii. The Fourth International Symposium on Computational Wind Engineering.*